2004 SUMATRA-ANDAMAN TSUNAMI SURVEYS IN THE COMORO ISLANDS AND TANZANIA AND REGIONAL TSUNAMI HAZARD FROM FUTURE SUMATRA EVENTS

E.A. OKAL
Department of Earth and Planetary Sciences, Northwestern University, Evanston, IL 60208, United States of America
e-mail: emile@earth.northwestern.edu

H.M. FRITZ
School of Civil and Environmental Engineering, Georgia Institute of Technology, Savannah, GA 31407, United States of America
e-mail: hermann.fritz@gtsav.gatech.edu

A. SLADEN
Laboratoire Risques Sismiques et Géologiques, Commissariat à l'Energie Atomique, F – 91297 Arpajon Cedex, France
Present address: Tectonics Observatory, Division of Geological and Planetary Sciences, California Institute of Technology, Pasadena, CA 91125, United States of America
e-mail: sladen@gps.caltech.edu

ABSTRACT

We present a total of 59 new data points of run-up of the 2004 Sumatra tsunami in the Comoros and Tanzania, surveyed in 2006 to 2008 by International Tsunami Survey Teams. Run-up along the northeastern coast of Grande Comore reached 6.9 m, surpassed only in the western Indian Ocean by the catastrophic values in Somalia (9 m). Tsunami inundation in Mayotte, and to a lesser extent Zanzibar, show considerable variations (from 1 to 4 m), attributed to the influence of the local structure of the reef surrounding these islands. By contrast, the unreefed islands of Anjouan and Moheli, and the mainland coast of Tanzania around Dar-es-Salaam, feature more consistent values in the 2 to 3 m range. The death toll in Tanzania is revised upwards to an estimate of at least 20. This new dataset complements the ones previously published for other western Indian Ocean shores, from Oman to South Africa.

We then use the MOST code to simulate the propagation on the high seas of both the 2004 tsunami, and of potential future tsunamis under scenarios of mega-earthquakes rupturing in the South Sumatra region; in particular, we consider the case of the great 1833 Mentawai earthquake, and of a probable future event releasing the strain accumulated on the 1833 rupture area but not released during the 2007 Bengkulu earthquake. While these studies are not carried to the full extent of run-up calculations at individual sites, they give a general estimate of expectable hazard, relative to 2004, under the relevant scenarios, at 19 offshore virtual gauges strategically located from Oman to South Africa. In general, the fragmentation of rupture expressed by the relatively moderate 2007 Bengkulu event leads to wave amplitudes smaller than in 2004 under the most probable future scenario, but at specific sites, including Port Elizabeth, unfavourable conditions such as a high tide could bring run-up to higher levels, with potential for serious destruction. Under the worst-case scenario of a rupture extending southeast of the 1833 fault zone, run-up greater than in 2004 could be expected at all sites south of the Comoros.

Introduction

The 2004 Sumatra-Andaman tsunami exported death and destruction across the Indian Ocean to its western shores. Yet, the amplitude of run-up, and with it the level of destruction, varied considerably, as documented for example along the eastern coast of Madagascar, where run-up ranged from 5 m in the south to an estimate of less than 0.5 m (tsunami not observed) in the central part of the coast (Okal et al., 2006a). Any understanding of these fluctuations requires a precise documentation of run-up on the largest possible dataset.

This paper comprises two parts. In Section two, we present the results of surveys carried out by International Tsunami Survey Teams (ITST) in the Comoro Islands and on Zanzibar and the Tanzanian mainland, which complement similar work performed in Oman, Yemen, Somalia, Kenya, the Mascarene Islands, Madagascar, and South Africa (Okal et al., 2006 a; b; c; Weiss and Bahlburg, 2006; Fritz and Borrero, 2006; Fritz and Okal, 2008; Okal et al., 2009). In particular, our work in Tanzania was motivated by the absence, to our best knowledge, of a systematic survey in that country, despite reports of at least ten casualties during the 2004 tsunami. In Section three, we further use numerical simulations to model the 2004 Sumatra-Andaman tsunami offshore of the surveyed coastlines,

doi:10.2113/gssajg.112.3-4.343

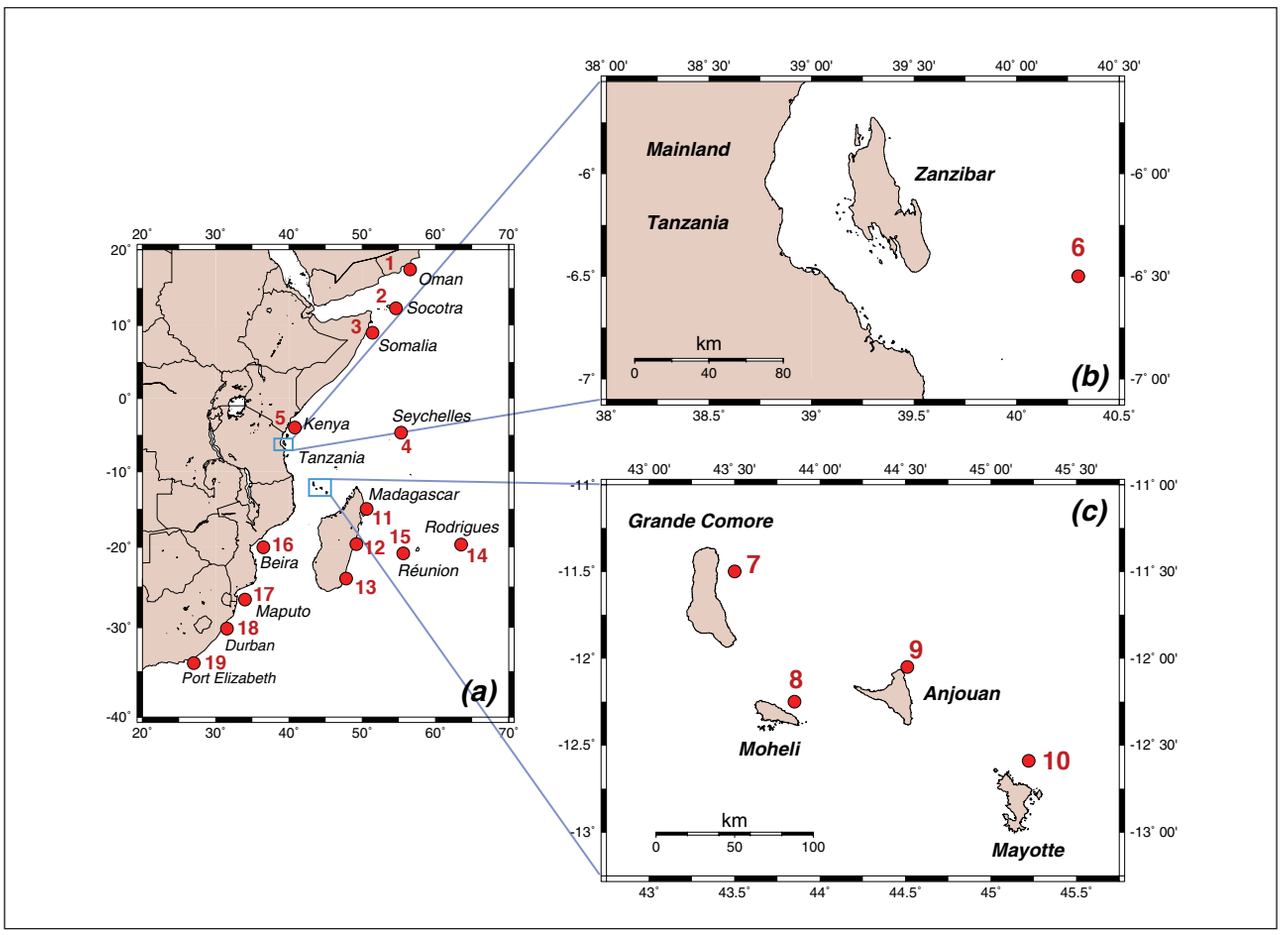

Figure 1. *(**a**) Location map of the areas surveyed along the coast of eastern Africa. The boxes show the areas outlined in (**b**) and (**c**). The dots (with names) identify the virtual gauges used in the tsunami simulation. (**b**) Close-up of the coast of Tanzania in the vicinity of Zanzibar Island, with virtual gauge 6. (**c**) Close-up of the Comoro archipelago, with virtual gauges 7 to 10.*

and to examine potential tsunami hazards to western Indian Ocean shores under a number of scenarios for future large earthquakes in the Sumatra subduction zone.

Surveys of the 2004 tsunami

Geological background: Comoros

The Comoros are a chain of four volcanic islands located at the northern end of the Mozambique channel separating Madagascar from southeastern Africa (see Figure 1). The morphology of the islands is that of Hawaiian volcanoes in various stages of growth and erosion, with the age of the edifices increasing southeastwards along the chain. The northernmost island, Grande Comore (1148 km^2), hosts the active Karthala volcano (rising to 2360 m a.s.l.), and is structurally reminiscent of the "Big Island" of Hawaii. The initiation of volcanism on the island of Moheli (211 km^2; 790 m a.s.l.) has been dated to 2.2 Ma, but the only ages (1.5 and 0.4 Ma) available for Anjouan (424 km^2; 1595 m a.s.l.) are likely post-erosional; the southeasternmost island, Mayotte (374 km^2; 660 m a.s.l.), strongly eroded and surrounded by a nearly continuous coral reef averaging 5 km in width, was dated at ~5.4 Ma (Hajash and Armstrong, 1972; Emerick and Duncan, 1982). Despite being rather regular, this age progression with distance (at least 5 cm/year) is too fast to be reconciled with the motion of either the Somalia plate (0.42 cm/year) or the Lwandle plate (0.17 cm/yr) over the mantle (Stamps et al., 2008). In other words, the rate of migration of volcanism in the Comoros would require excessive rates of spreading across the African Rift. For that reason, Gripp and Gordon (2002) discarded the Comoros chain (and incidentally, the Réunion-Mauritius one) from their global study of the motion of young hotspot chains over the mantle.

The islands of Grande Comore, Anjouan and Moheli comprise the Republic of the Union of the Comoros, while Mayotte remains a commonwealth of the French Republic.

Geological background: Tanzania

The provinces surveyed, coastal Tanzania in the vicinity of Dar-es-Salaam and Zanzibar, belong to one of the oldest margins of continental Africa, which broke away from Australia in the Late Jurassic (Müller et al., 2008), and are described as being presently part of the Somalia

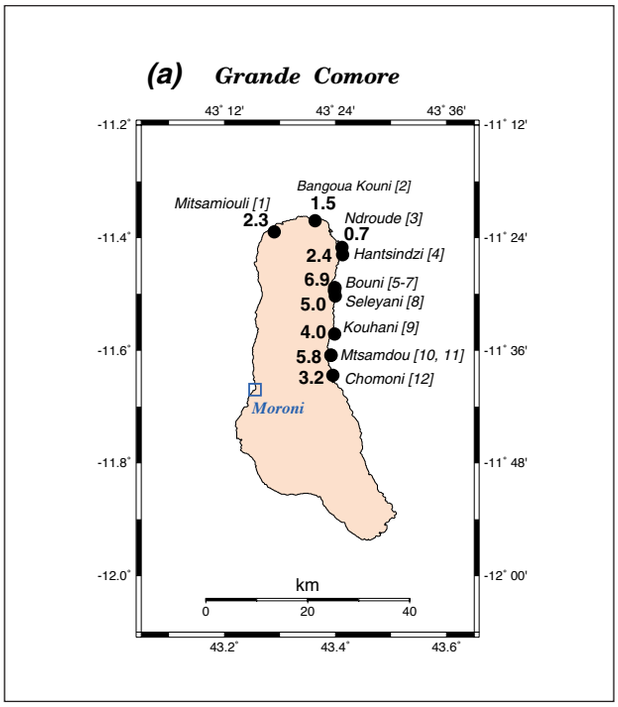

Figure 2. *Maps of the results of the tsunami survey. (**a**) Grande Comore; (**b**) Anjouan; (**c**) Moheli; (**d**) Mayotte; (**e**) Zanzibar; (**f**): Mainland Tanzania. On each frame, the localities surveyed are shown as solid dots, and numbered in italicized brackets e.g., [1], according to Table 1. Run-up values (in m) are shown as bold numbers (e.g., **3.2**). When several values were obtained at two nearby sites, only the largest one is mapped. The inverted triangle on Frame (e) refers to a flow depth on the barrier reef. Open squares denote major cities.*

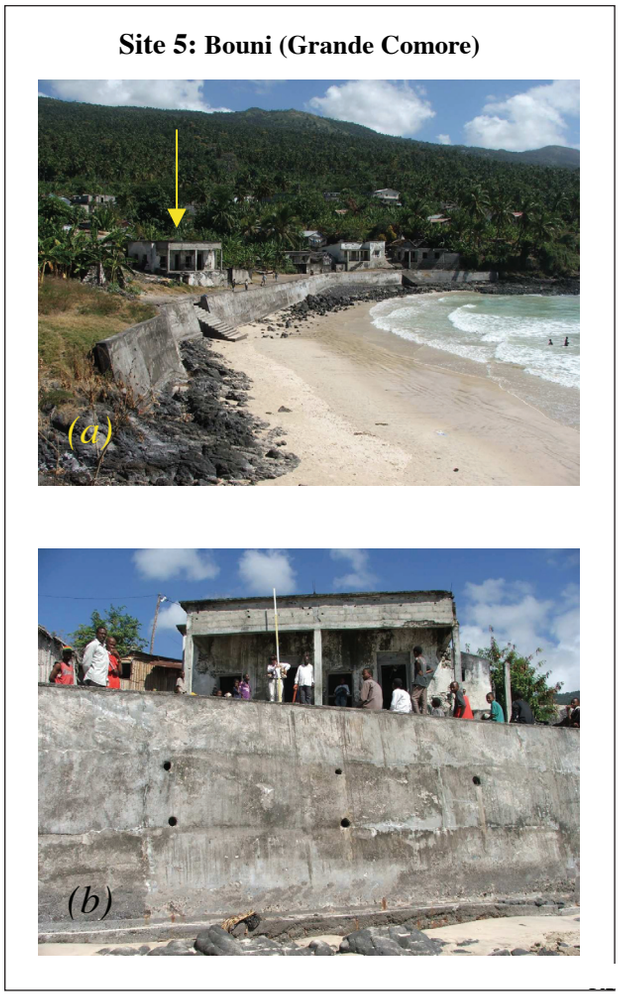

Figure 3. *Tsunami survey at site 5 (Bouni, Grande Comore). (**a**): Beachfront view of the village of Bouni, where one of the greatest run-ups (6.0 m; tide-corrected) was recorded. The tsunami reached the floor of the building marked with the arrow (which serves as a mosque). Note the seawall in front of the building. (**b**) Close-up as seen from the beach during surveying. Photographs: H.M. Fritz.*

plate (Stamps et al., 2008). The area of Dar-es-Salaam constitutes the central mainland coastal region, and is characterized by estuarine and marine sedimentary units, several km thick, and of Late Cretaceous and Tertiary ages (Kent et al., 1971).

Zanzibar (1651 km^2; maximum elevation: 120 m) is the largest island off the coast of eastern Africa, from which it is separated by a channel as shallow as 50 m. The island is covered mostly with Quaternary reefal limestones, with some Pliocene soft sandstones in its western part (Kent et al., 1971). It is fringed by a well-developed coral reef, essentially continuous except on a section of the western coast home to the main settlement of Zanzibar City.

Logistics and methods

Field work was carried out in September 2006 on Mayotte and at the northernmost sites on Grande Comore, in July 2007 at the remaining sites on Grande Comore, on Anjouan and Moheli, and in September 2008 at the Tanzanian sites.

The surveying teams used the conventional methods described in previous reports (e.g., Synolakis and Okal, 2005). At each site, eyewitnesses of the tsunami were identified and questioned as to the penetration of the waves, and their sequence, i.e., the relative amplitudes of the several wavetrains, the duration of the phenomenon and its polarity (inundation or withdrawal by the first wave). Based on their testimony, which was videotaped for permanent archival (only during the Comoro surveys), conventional topographic methods were used to measure run-up (or occasionally flow depth) and inundation. We define *inundation* as the maximum horizontal extent of the penetration of the tsunami, *run-up* as the altitude of the point of maximum penetration, and *flow depth* as the height of the wave as it crossed the shoreline (e.g., Synolakis and Okal, 2005). Run-up values were corrected for tides by adding the difference between the height of the tide during the survey and at the arrival time of the tsunami on 26 December 2004.

The full dataset of results are listed in Table 1 and mapped on Figures 2a–f.

Table 1. 2004 Indonesian tsunami survey dataset in the Comoro Islands and Tanzania

Site	Latitude	Longitude	Date and Time	Run-up (m)		Location
Number	(°S)	(°E)	Surveyed (GMT)	Raw	Tide-corrected	
Grande Comore						
1	11.38980	43.28947	13-Sep-2006 08:22	2.80	2.30	Mitsamiouli
2	11.36983	43.36338	13-Sep-2006 09:25	2.52	1.50	Bangoua Kouni
3	11.41733	43.41175	13-Sep-2006 10:25	1.75	0.65	Ndroudé, Ile de la Tortue
4	11.43047	43.41280	13-Sep-2006 11:07	3.60	2.40	Hantsidzi
5	11.48882	43.39847	25-Jul-2007 07:15	5.80	6.00	Bouni Mosque 1
6	11.48938	43.39917	25-Jul-2007 07:35	6.70	6.90	Bouni Mosque 2
7	11.49425	43.39805	25-Jul-2007 07:50	5.80	6.00	South of Bouni, Road
8	11.50363	43.39957	25-Jul-2007 08:15	4.70	5.00	Séléyani
9	11.57127	43.39837	25-Jul-2007 09:00	3.50	4.00	Kouhani
10	11.60860	43.39197	25-Jul-2007 09:45	5.10	5.60	Mtsamdou – Hill
11	11.60905	43.39170	25-Jul-2007 09:55	4.30	5.80	Mtsamdou – Seawall
12	11.64477	43.39508	25-Jul-2007 10:20	2.70	3.20	Chomoni
Anjouan						
13	12.26172	44.53260	26-Jul-2007 09:00	1.20	1.70	Domoni – South
14	12.25923	44.53119	26-Jul-2007 09:52	1.40	1.90	Domoni – North
15	12.20240	44.52037	26-Jul-2007 10:20	1.90	2.50	Bambao
16	12.17223	44.50653	26-Jul-2007 10:45	2.10	2.70	Ongoni
17	12.12090	44.48885	26-Jul-2007 11:15	1.70	2.30	Hajoho
18	12.19175	44.23317	26-Jul-2007 13:50	2.90	2.90	Bimbini
19	12.15693	44.41515	27-Jul-2007 04:55	2.90	2.10	Mirontsi
Moheli						
20	12.25638	43.67012	28-Jul-2007 06:15	3.20	2.20	Gnambo-Yamaore
21	12.26802	43.70543	28-Jul-2007 06:52	3.80	2.80	Mtakoudja
22	12.27940	43.73847	28-Jul-2007 07:19	3.10	2.10	Fomboni Ouest
23	12.29015	43.75282	28-Jul-2007 07:37	4.20	3.80	Bangoma – Port
24	12.30595	43.77660	28-Jul-2007 08:00	3.60	2.80	Djoyézi
25	12.33963	43.84248	28-Jul-2007 08:32	3.50	3.00	Hagnamouada
26	12.30400	43.63465	28-Jul-2007 10:15	3.10	3.50	Miringoni
Mayotte						
27	12.74395	45.22052	15-Sep-2006 12:40	3.20	2.65	Majikavo-Koropa
28	12.73467	45.20828	15-Sep-2006 13:05	4.60	4.05	Koungou, East
29	12.73480	45.20755	15-Sep-2006 13:15	3.50	2.95	Koungou, East
30	12.69002	45.11142	16-Sep-2006 05:25	2.00	2.00	Mtsangamboua
31	12.68162	45.08042	16-Sep-2006 06:10	2.80	2.95	Mtsahara
32	12.68767	45.07335	16-Sep-2006 06:36	0.80	1.00	Hamjago
33	12.69817	45.06762	16-Sep-2006 07:25	1.00	1.25	Mtsamboro
34	12.71112	45.05005	16-Sep-2006 07:53	2.60	2.90	Mtsangadoua
35	12.72528	45.05615	16-Sep-2006 08:15	2.10	2.40	Acoua
36	12.83640	45.11225	16-Sep-2006 09:20	2.20	2.45	Chiconi
37	12.84942	45.09867	16-Sep-2006 09:42	1.10	1.30	Sada
38	12.90602	45.07742	16-Sep-2006 10:44	3.20	3.30	Bouéni
39	12.92863	45.10238	16-Sep-2006 11:15	1.30	1.30	Mzouazia
40	12.96285	45.17673	16-Sep-2006 12:30	2.40	2.20	Moutsamoudou
Zanzibar						
41	5.86848	39.35385	02-Sep-2008 07:42	3.15	2.90	Matemwe Beach
42	5.72238	39.30228	02-Sep-2008 08:55	1.50	1.50	Nungwi Aquarium
43	5.99612	39.38150	02-Sep-2008 10:50	<1.50	<1.50	Kiwengwa – Estimate
44	6.10492	39.42708	02-Sep-2008 11:50	<1.0	<1.50	Uroa Tamarind Hotel
45	6.15563	39.43705	02-Sep-2008 12:45	1.85	2.65	Chwaka Bay Resort Hotel
46	6.26048	39.53660	03-Sep-2008 07:30	1.00	1.00	Paje – Flow depth on reef
47	6.18032	39.53105	03-Sep-2008 08:10	3.70	2.40	Dongwe Restaurant "The Door"
48	6.34270	39.55717	03-Sep-2008 09:20	4.45	3.25	Jambiani Red Monkey Lodge
49	6.45608	39.47358	03-Sep-2008 10:15	<1.5	<1.50	Kizimkazi

Table 1. continued

Site Number	Latitude (°S)	Longitude (°E)	Date and Time Surveyed (GMT)	Run-up (m) Raw	Run-up (m) Tide-corrected	Location
Mainland Tanzania						
50	6.44017	38.91025	04-Sep-2008 09:30	3.00	3.00	Bagamoyo – Fishing harbor
51	6.42835	38.90360	04-Sep-2008 10:15	3.00	3.00	Bagamoyo – Oceanic Bay Resort
52	6.47287	38.97017	04-Sep-2008 11:45	3.50	2.50	Mbegani – Institute of Fisheries
53	6.65455	39.21232	04-Sep-2008 13:05	2.50	3.30	Silver Sands Resort
54	6.67942	39.22458	05-Sep-2008 07:25	4.00	3.00	Beachcomber Hotel
55	6.69817	39.22763	05-Sep-2008 07:50	3.50	3.00	Mbezi Beach
56	6.66848	39.21867	05-Sep-2008 08:40	3.75	3.50	Konduchi Beach
57	6.81845	39.30085	05-Sep-2008 11:13	2.90	2.40	Dar-es-Salaam Fishing Harbor and Ferry
58	6.85103	39.36145	05-Sep-2008 12:50	2.40	2.40	Kipepeo Beach
59	6.86335	39.41087	05-Sep-2008 13:25	2.75	2.85	Kim Beach – at berm

Grande Comore; Figure 2a

Surveying was conducted at 12 points along the northeastern part of the island, since the tsunami went mostly unnoticed on the western shore, which incidentally is the most populated, with the capital city of Moroni. Sites 1 to 4 were visited by E.A. Okal on 13 September 2006, and sites 5 to 12 by Okal and Fritz on 25 July 2007. Significant run-up was measured along the 15 km Bouni–Mtsamdou segment of the coast, with values reaching 6.9 m at site 6 in Bouni. With the exception of Somalia, located in the lobe of source directivity (Ben-Menahem and Rosenman, 1972), these values are the highest surveyed on the western shore of the Indian Ocean (Fritz and Borrero, 2006; Okal et al., 2006a; b; c; Weiss and Bahlburg, 2006), and they are also comparable to a point surveyed by Fritz and Okal [2008] at Shazhor, on the easternmost part of Socotra. However, inundation at sites 5 to 12 never exceeded 50 m, and in particular the large run-up values at Bouni were measured behind a seawall at site 5 (6.0 m; Figure 3), and up a steep hill at nearby site 6 (6.9 m). By contrast, the waves penetrated as much as 700 m inland at Xaafuun, Somalia, and 132 m at Shazhor, Socotra. This difference in coastal morphology helped reduce the damage caused by the tsunami on Grande Comore, as all settlements were located out of harm's way. While no human casualties were deplored, a number of sheep and goats were swept away in Séléyani (site 8), and at least five canoes were washed away in Bouni (site 5).

Anjouan; Figure 2b

Anjouan was visited by Okal and Fritz on 26 July 2007, with the last point (Mirontsi; site 19) surveyed the next day. By contrast to Grande Comore, the tsunami had limited run-up amplitudes (ranging from 1.7 to 2.9 m) at the seven locations surveyed on Anjouan. The general steepness of the eastern shore of Anjouan provided a natural shelter against the waves, with the exception of Hajoho in the north, where the wave penetrated 56 m inland at the mouth of a river; it remained benign since the local settlements are located a further 100 m inland.

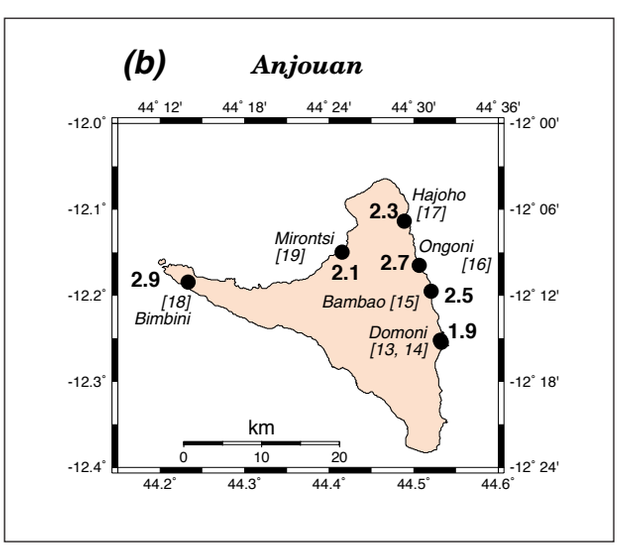

Figure 2. *(**b**) Anjouan*

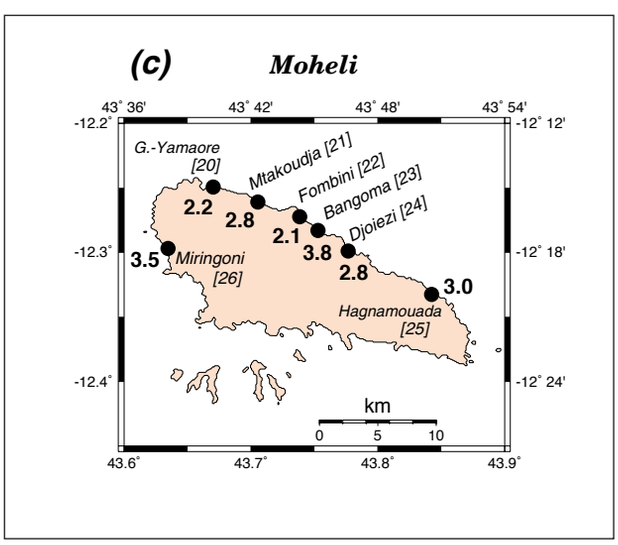

Figure 2. *(**c**) Moheli*

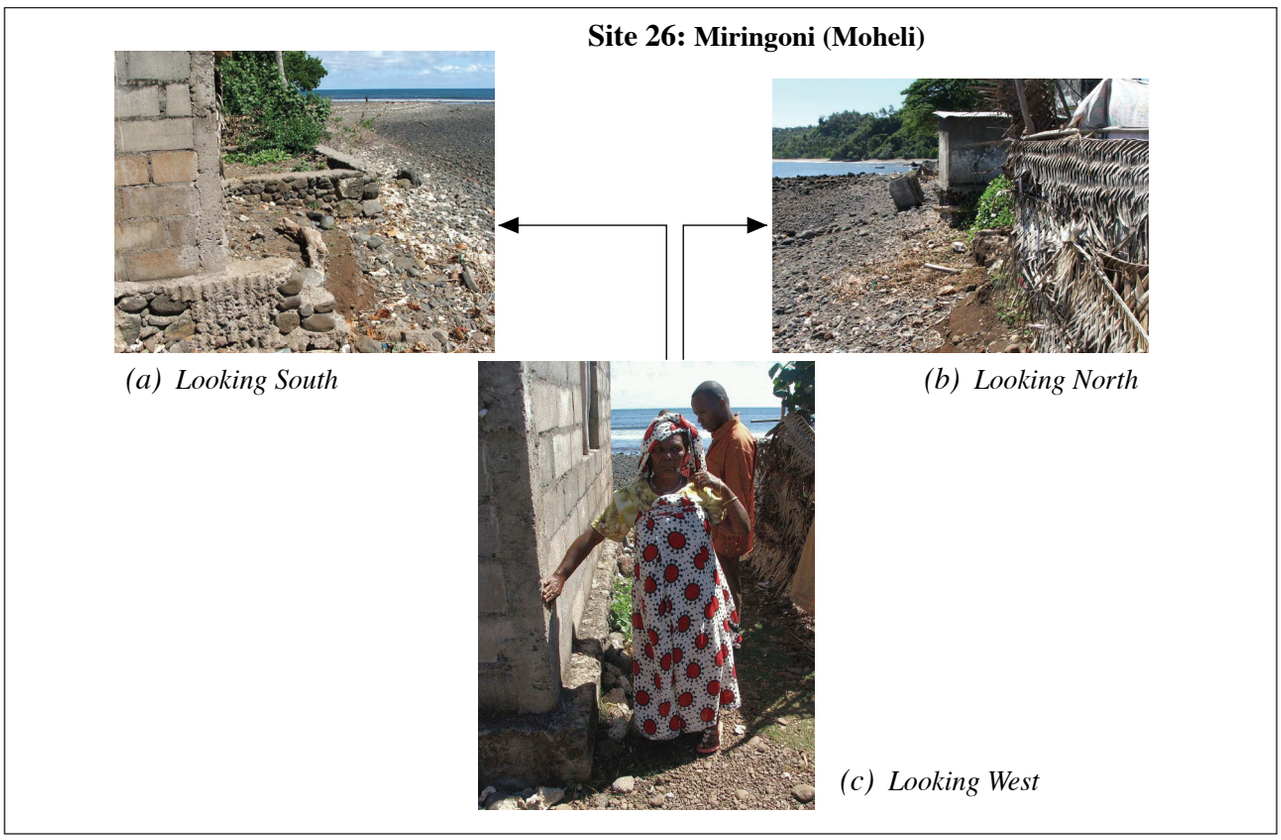

Figure 4. *Evidence of tsunami damage at site 26 (Miringoni, Moheli). (**a**) Remnants of wall built in front of house destroyed by the tsunami. This view looks south along the beach from the passage shown on frame (c). (**b**) Same as (a), looking north along the beach, showing wall destroyed by tsunami, and replaced by palm partition. Note large block, part of wall foundation, in distance. (**c**) Interviewed witness standing in passageway (looking west towards the sea) along house flooded by tsunami. Her right hand extends to a level representative of that reached by the waves inside the house. Photographs: H.M. Fritz*

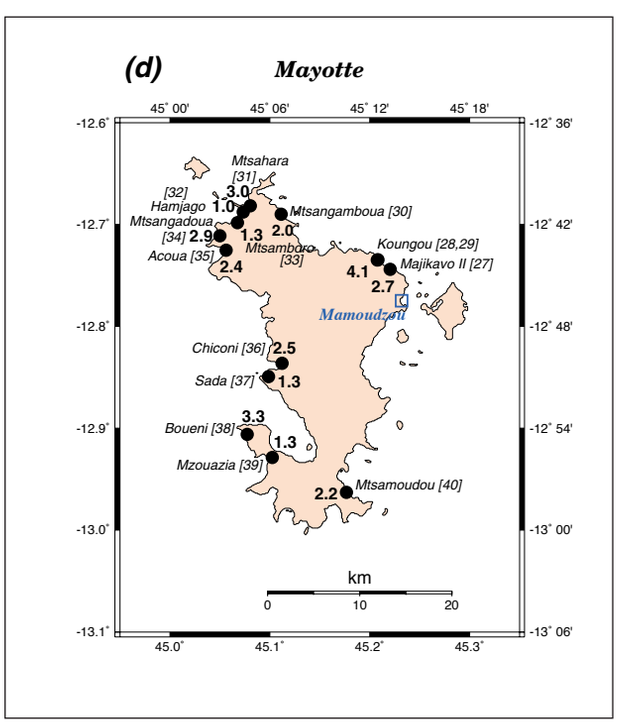

Figure 2. *(**d**) Mayotte*

Moheli; Figure 2c

Moheli was visited by Okal and Fritz on 28 July 2007. The island presents a remarkably linear coastline on its northern shore, essentially perpendicular to the incident direction of the tsunami, and surveyed run-up was stable along that coast (2.1 to 3.8 m). Only one site could be visited on the southwest part of the island, with surveyed run-up not significantly different (Miringoni, site 26; 3.5 m). At that location, we interviewed a witness who told us that she had been napping during the event, and was awakened by a phone call from a relative (at an unknown location), warning her of the tsunami, but she did not evacuate. The waves destroyed a wall in front of her house, and flooded the house up to her mattress, fortunately inflicting no harm, at a total run-up height of 3.5 m (Figure 4). Despite its happy ending, this story points to an inadequate response to an apparent personal warning; it constitutes an obvious example of the necessity to keep the population aware of tsunami hazard through an educational effort.

Mayotte; Figure 2d

Mayotte was visited by Okal, Fritz and Sladen on 15 to 16 September 2006. Run-up values at the 14 sites

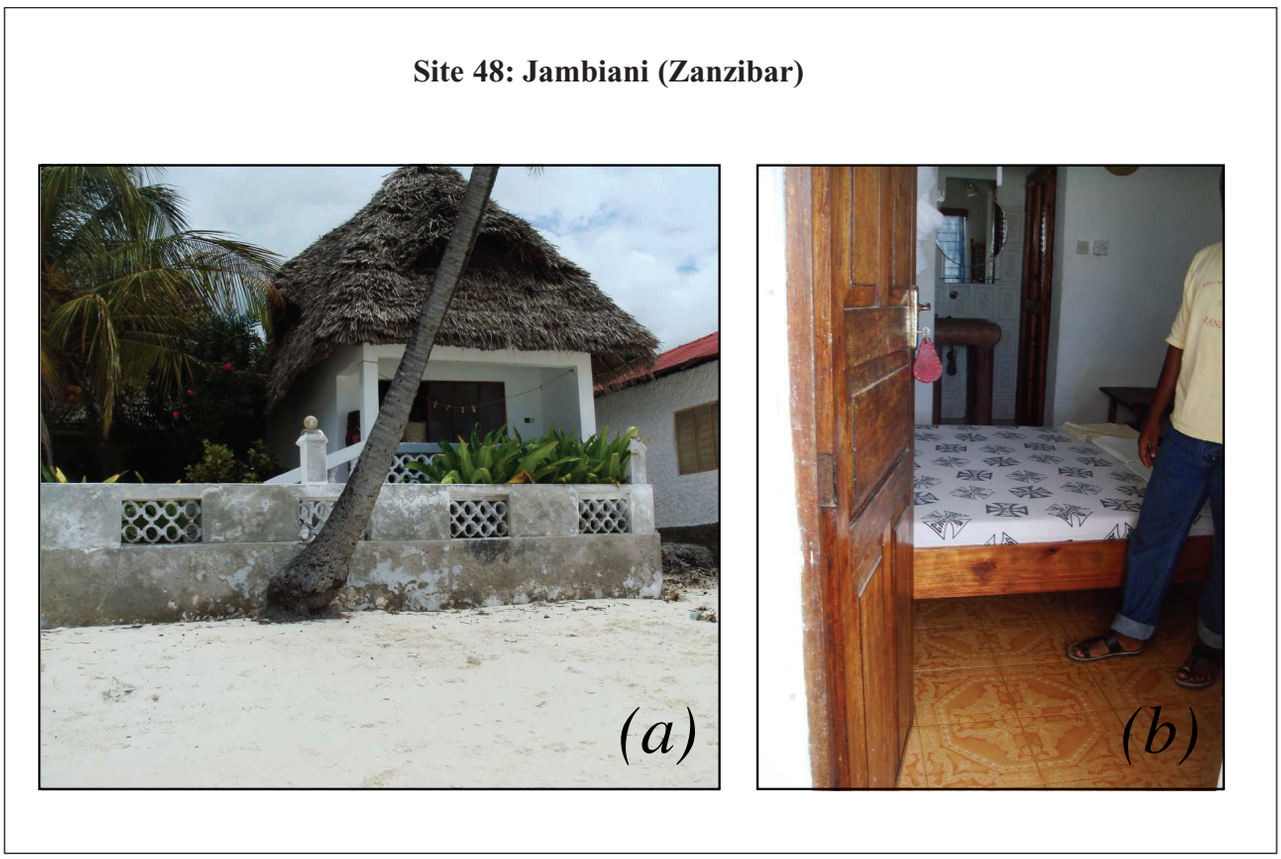

Figure 5. *Site 48; Red Monkey Lodge, Jambiani, Zanzibar. (**a**) View of bungalow inundated by tsunami. The foot of the wall in front of the structure represents the storm wave line. (**b**) Interior of bungalow where the tsunami reportedly moved the bed around the room. Photographs: E.A. Okal.*

surveyed on the island range from 1.0 m at Hamjago to 4.1 m at Koungou East. At several locations on the north coast, between sites 33 and 34, witnesses reported that they had not noticed any inundation. This large scatter may be attributable to irregularities in the structure of the coral reef surrounding Mayotte. We note that similar effects were described qualitatively by Okal et al. (2006*c*) in Rodrigues during the 2004 Sumatra tsunami, and by Okal and Hébert (2007) on the Polynesian islands of Tubuai and Raivavae, during a survey of the 1946 Aleutian tsunami.

Zanzibar; Figure 2e

The eastern shore of the island was visited by Okal on 02 to 03 September 2008. As in the case of Mayotte, the island is reefed and run-up values varied significantly and somewhat erratically from a maximum of 3.3 m at Jambiani (site 48) to an estimated minimum of less than 1.5 m at Uroa (site 44) where the tsunami did not reach higher than average high tide. However, the reef is generally closer to the dry land (typically 1.5 km) than at Mayotte (typically 5 km). We note that high run-up values (at Jambiani and Dongwe) occurred at sites featuring a wide channel through the barrier reef; in particular, the restaurant at Dongwe (site 47) is named "The Door" to express this opening into the

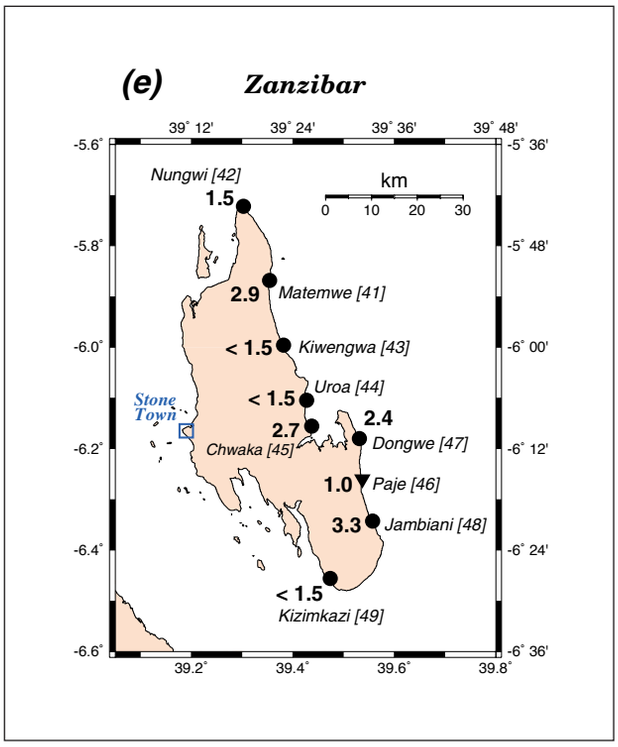

Figure 2. *(**e**) Zanzibar*

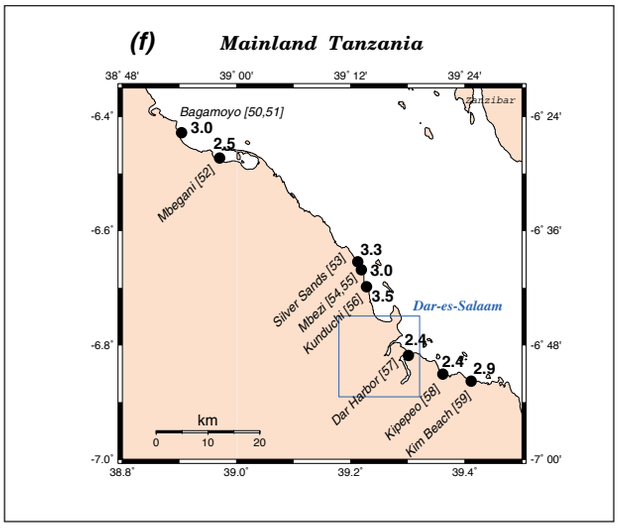

Figure 2. *(**f**) Mainland Tanzania.*

ocean, in an area where the reef is also generally closer to the coast (0.9 km). At Jambiani, the wave penetrated during high tide into a bungalow (located approximately 1 m above the storm wave line), where it reportedly moved the bed around the room (Figure 5); one dhow (fortunately with no one aboard) broke its moorings and was lost.

An interesting report was obtained at site 46 (Paje) where our witness (the hotel manager) reported an essentially undetected wave at the resort itself, while his son, a diving instructor who was walking tourists on the reef, exposed during low tide (around 13:30 GMT +3), experienced sudden waist-deep flooding upon arrival of the tsunami. We interpret this report as a flow depth of 1 m on the reef, distant 1.6 km from the beach at that location.

It is noteworthy that three witnesses in Zanzibar provided independent and unsolicited reports of feeling a weak earthquake preceding the tsunami sequence. We were unable to associate these reports with catalogued events in the area. Rather, we explore the possibility that the witnesses felt *T* phases, i.e., seismic conversions of hydroacoustic waves from the mainshock; their expected arrival time would be 05:10 GMT +3, 7.5 hours before the tsunami. Indeed, *T* phases from the 2004 Sumatra mainshock were felt in the Maldives (Synolakis and Kong, 2006) and on Diego Garcia (Robertson et al., 2005). In the absence of seismic records at coastal locations in Tanzania, it is difficult to estimate the possible amplitude of converted *T* phases on Zanzibar, but we turned to the closest available record of a *T* phase from the Sumatra mainshock, at Kilima Mbogo, Kenya (KMBO), a station located 370 km from the nearest coastline. It features a peak ground acceleration of 10^{-4} cm/s^2 in the 1 to 6 Hz bandwidth. By contrast, at Rivière de l'Est, Réunion, only 7 km from the shoreline, the *T* phase acceleration is only double that value. Since high-frequency seismic waves converted from *T* phases are strongly attenuated over

Site 56: Konduchi Beach (Tanzanian Mainland)

Figure 6. *(**a**) Location of house reportedly destroyed by the tsunami at Konduchi Beach (Site 56). (**b**) The witness (centre) shows remnants of materials described as representative of its construction. Photographs: E.A. Okal.*

continental paths, the record at KMBO requires, at least qualitatively, that hydroacoustic phases of exceptional intensity must have reached the Kenyan shore, and thus most probably also Zanzibar, only 350 km further south, lending support to the association of the felt reports with the arrival of the *T* phase from the main shock. The timing, "in the morning" according to two of our witnesses, is vague enough not to invalidate this interpretation. We note however that another witness spoke of an earthquake felt "after the tsunami", a report clearly impossible to associate not only with the *T* phases, but also more generally with the other reports of felt tremors.

Mainland Tanzania; Figure 2f.

Ten sites were visited by E.A. Okal on 04 and 05 September 2008 within 70 km of Dar-es-Salaam. Run-up values were found consistently in the 2.4 to 3.5 m range. At site 56 in Konduchi Beach, a house was reportedly destroyed by the tsunami between 15:00 and

18:00 (GMT +3) at a tide-corrected elevation of 3.5 m. It was described to us as being made of "stone, coral and cement", but its exact construction could not be further asserted (Figure 6).

At site 57, in Dar-es-Salaam harbour, fishing boats broke their moorings and were swept up the beach or inside the inner harbour. The operation of the cross-harbor ferry was interrupted due to strong currents. Collisions between dhows inflicted damage to several boats. This took place "in the evening", suggesting the influence of high-frequency components of the tsunami, in a pattern reminiscent of the incidents in Réunion and Madagascar (Okal et al., 2006a; c).

Casualties

Contrary to an early oral report, no casualties could be confirmed on any of the four islands of the Comoro archipelago. By contrast, on the Tanzanian mainland, eight casualties were reported and confirmed by several witnesses in the vicinity of site 55 (Mbezi Beach), near a river estuary. The victims were teenagers swimming in the sea, who were swept away, presumably during an ebbing phase by strong currents enhanced by the presence of the estuary. Two additional casualties were confirmed at site 58 (Kipepeo Beach, east of Dar-es-Salaam); according to our witness (the manager of a local resort), the victims were tourists visiting from the hinterland, reveling in shallow water, but unable to swim, who were overwhelmed by the increased flow depth during an inundation phase. There were unconfirmed reports of additional casualties at Bagamoyo (site 50) and in Dar-es-Salaam harbour (site 57).

More casualties, reportedly two with at least ten injuries, were deplored in the Rufiji district, where the Rufiji River discharges into the ocean through a large delta, approximately 120 km South of Dar-es-Salaam. The area is difficult to access and could not be visited during the survey. These numbers suggest that at least 15 people lost their lives along a 200 km stretch of coastline. It is probable that the death toll for the whole 700 km Tanzanian coastline exceeded twenty, which would make it the second highest in Africa after Somalia (300 deaths; Fritz and Borrero, 2006).

Characteristic of the waves: timing, number, relative strengths

We systematically asked our witnesses for their recollections of the principal characteristics of the wavetrains: Approximate arrival time, number of wavetrains, sequence of amplitudes, and timing between waves. In general, their responses were somewhat imprecise, which could be expected given that some of them were interviewed 3.5 years after the event. In both the Comoros and Tanzania, the average arrival time reported to us was 14:00 ± 1:30, GMT +3 (rounded up to the nearest half-hour); this corresponds to a travel-time of 10 hours, in good agreement with the 9.5 hours predicted by simulation models (Titov et al., 2005). No consensus arose on the number of large waves, described as anywhere between one and four in the Comoros, two and four in Tanzania, with a number of witnesses mentioning "tens of waves", thereby probably referring to the prolonged agitation of the sea rather than to large scale inundation. On the other hand, most of our witnesses described the first wave as the biggest one, in contrast to numerical simulations. Combined with the slight delay in arrival, this could suggest that the true first (and predicted smaller) positive wave may have gone unnoticed. The period of the waves was described as anywhere between two and 30 minutes, but our experience with previous surveys (Synolakis and Okal, 2005) indicates that the perception, and especially the memorisation, of time intervals by witnesses remains far from quantitative and thus unreliable. Neither was a consensus obtained on the polarity of first motion (an inundation or a recess of the sea), which again could be an artifact of the occasional failure to detect the first and smaller wave, expected positive oceanwards in the subduction geometry (Okal, 2008).

Hydrodynamic simulations

In the context of our observations of a strong variability of run-up along the western shores of the Indian Ocean, we use basin-wide hydrodynamic tsunami simulations to explore the influence of far-field propagation on the wave height expected in deep water near the shorelines, under scenarios modeling both the 2004 event and expectable future mega-thrust earthquakes

Table 2. Sources used in the numerical simulations

Number	Source	Centroid		Fault parameters			Moment	Focal mechanism		
		(°N)	(°E)	Length L (km)	Width W (km)	Slip Δu (m)	(10^{29}dyn*cm)	ϕ (°)	δ (°)	λ (°)
I.a	2004.a	3.3	94.6	382	150	11.5	3.2	318	6.4	94
I.b	2004.b	7.0	93.8	818	150	12.4	7.3	355	7	109
I.	Sumatra-Andaman 2004			1200	150		10.5			
II.	Mentawai 1833	–3.0	99.7	550	175	13	6.0	322	12	90
III.	Bengkulu 2007	–4.4	101.6	190	95	5.6	0.5	329	8	100
IV.	1833 post–2007	–3.7	100.6	350	175	6.0	1.9	322	12	90
V.	IV + South	–4.25	100.7	900	175	8.0	6.0	322	12	90

In all cases, the depth to the top of the rupture is taken as 10 km.

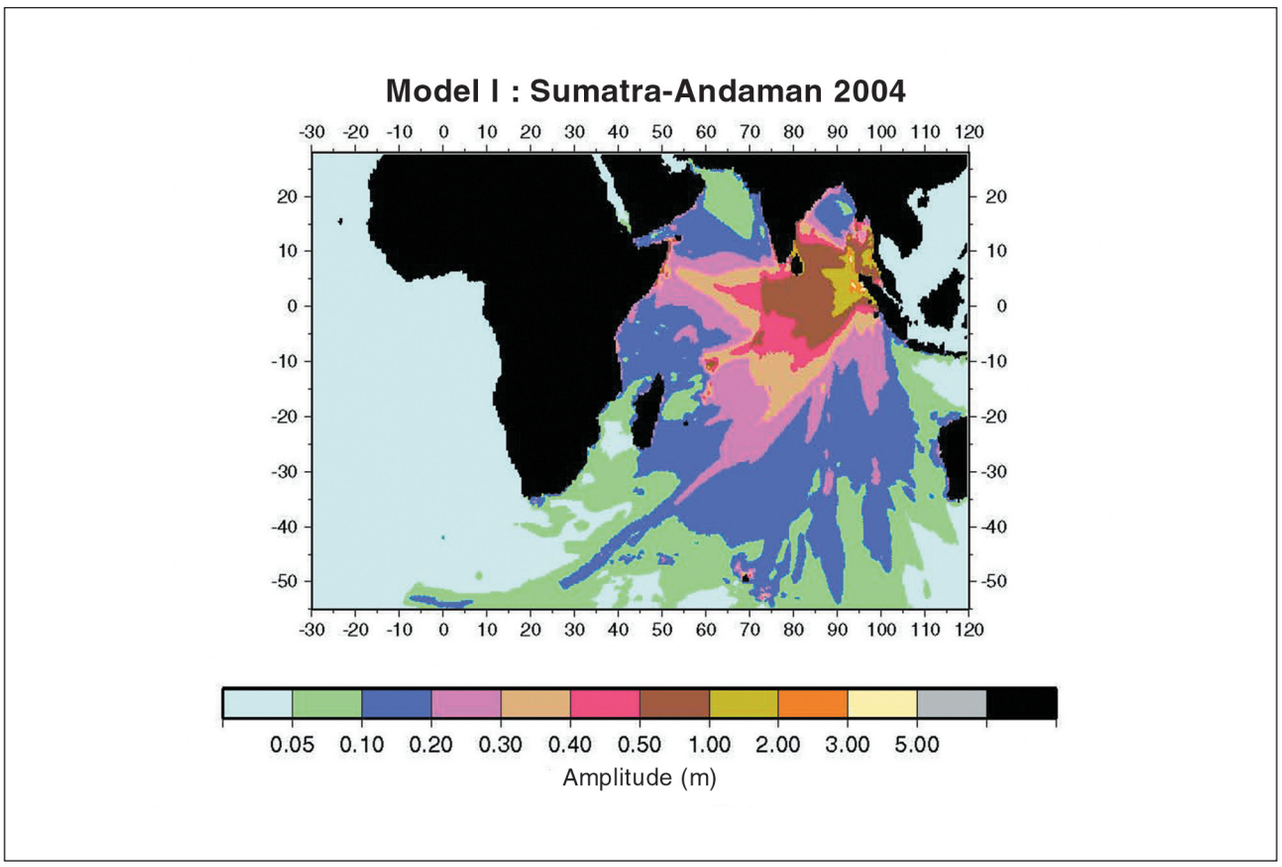

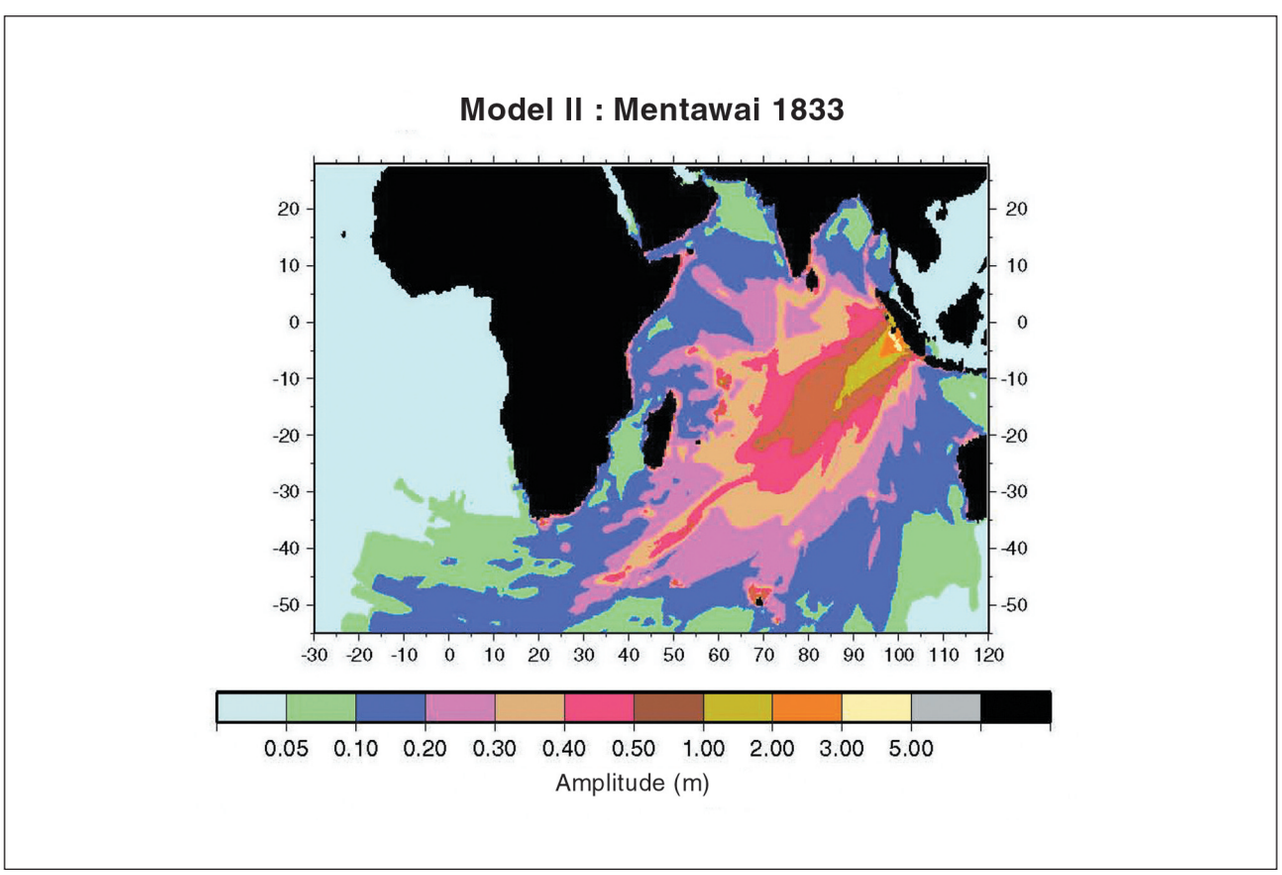

Figure 7. *Fields of maximum amplitudes resulting from the numerical simulations of the five models considered in this study and listed in Table 2. The palette is common to all five plots.*

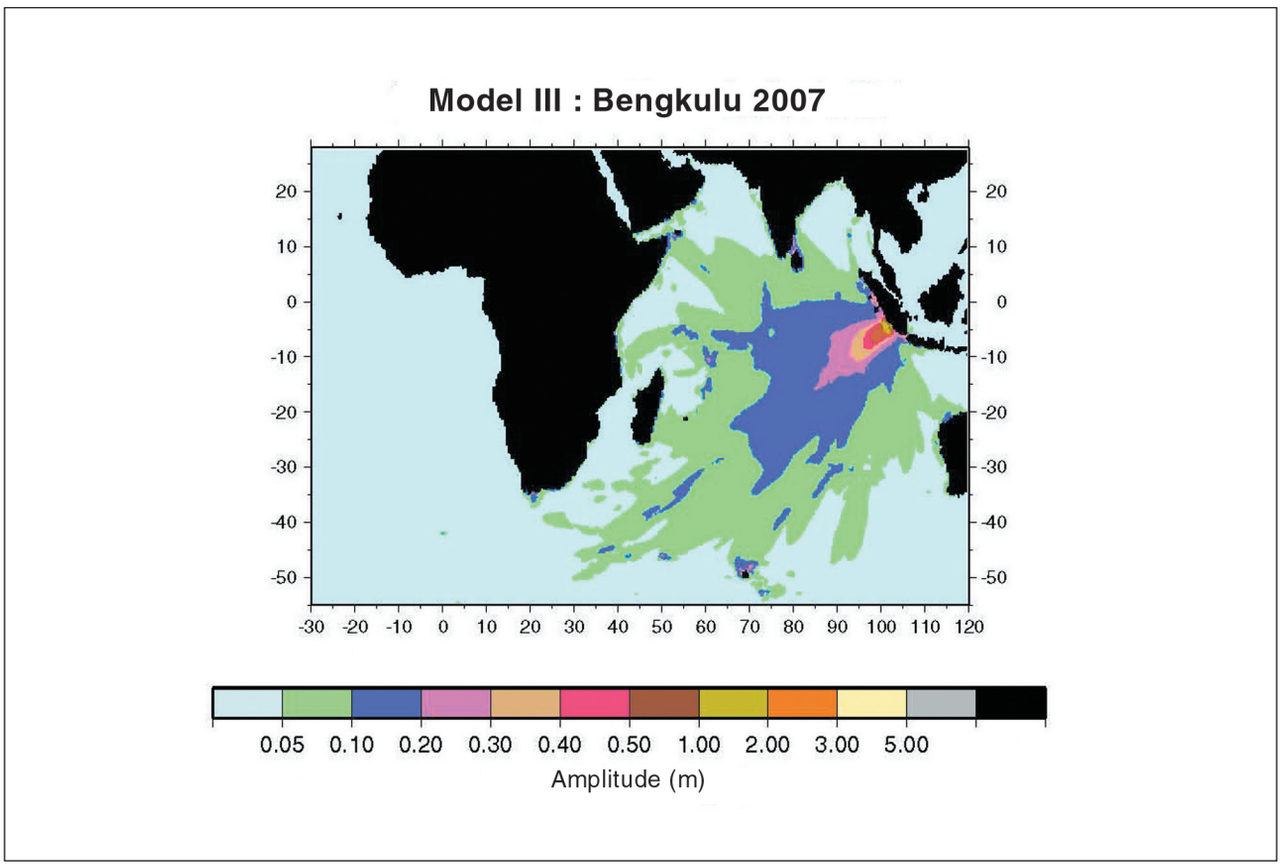

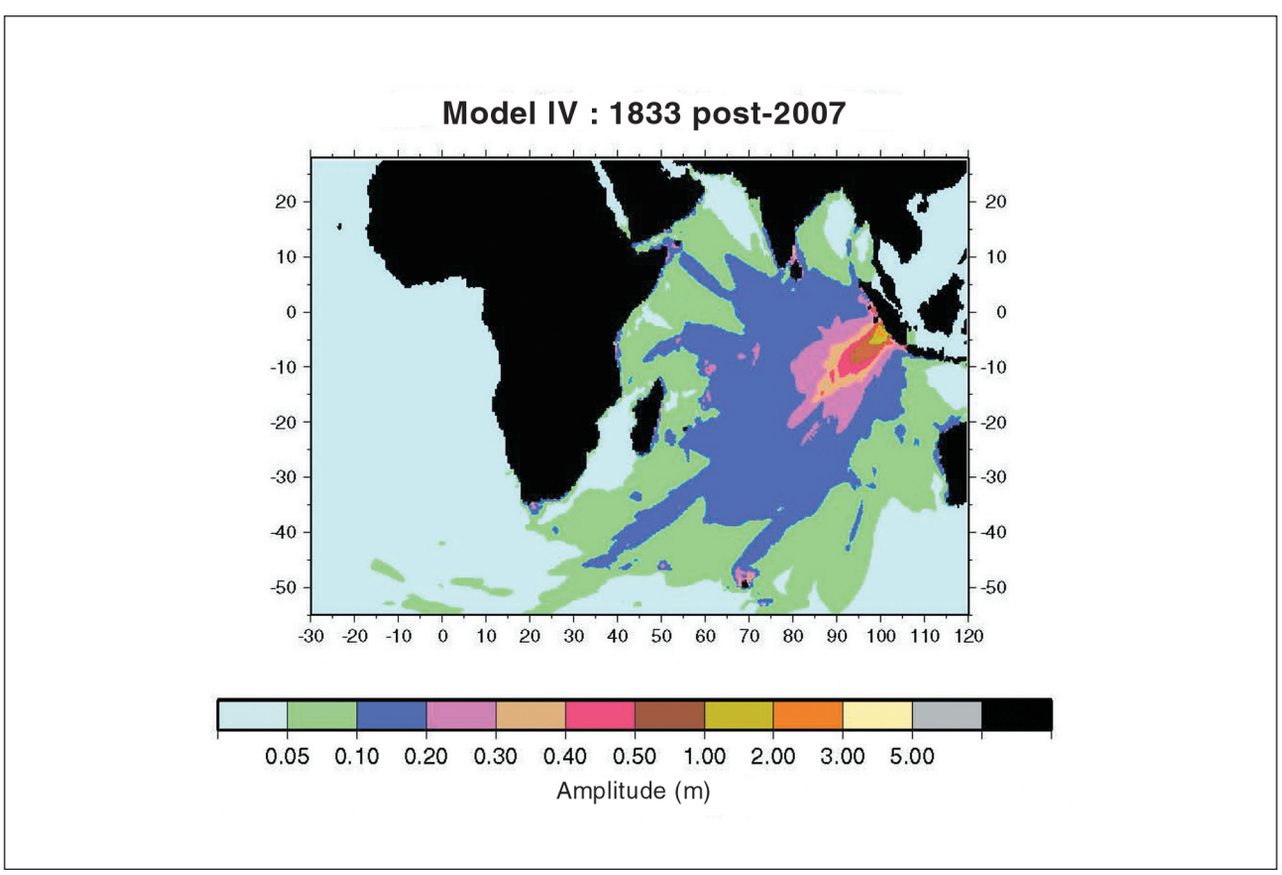

Figure 7. *continued.*

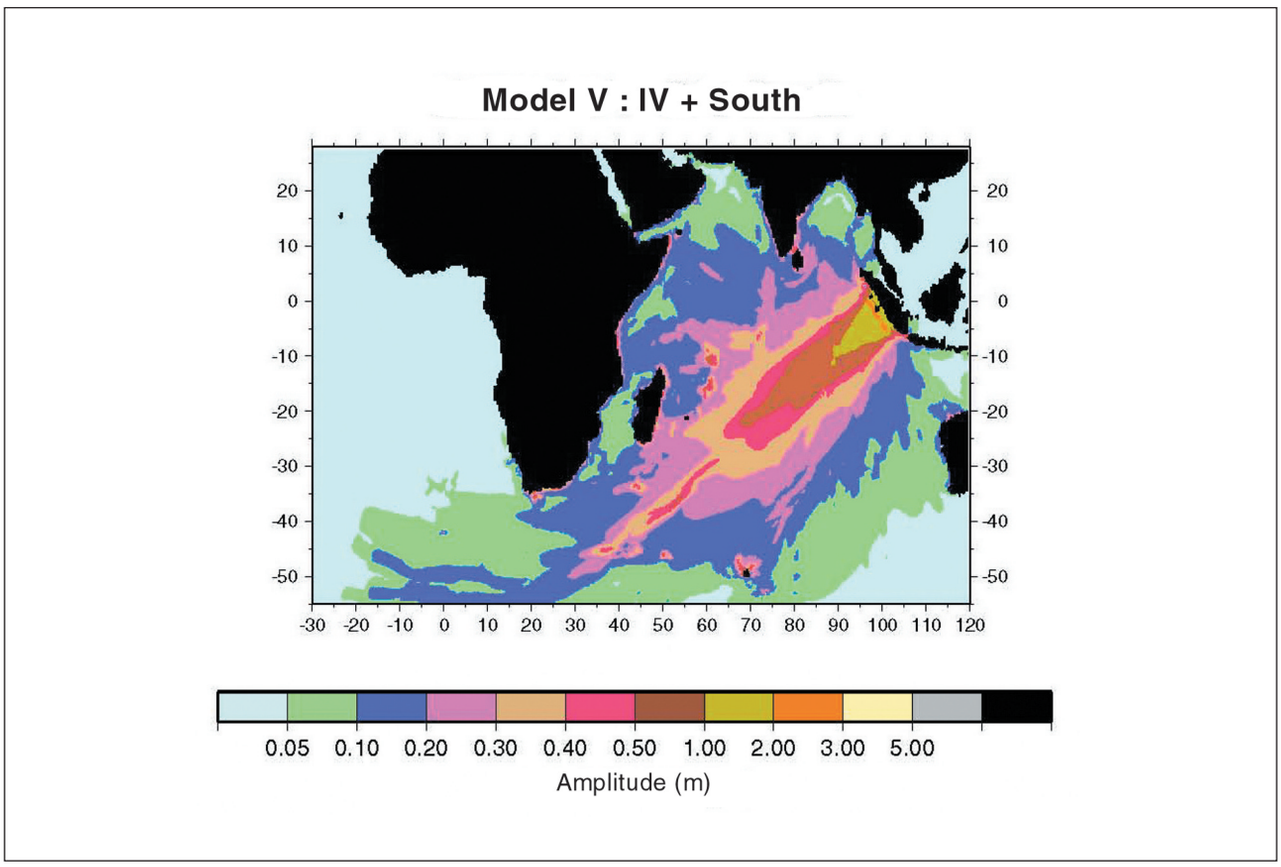

Figure 7. *continued.*

at the Sumatra trench. Our simulations use the MOST code (Titov and Synolakis, 1998), which solves the full non-linear equations of hydrodynamics under the shallow water approximation, using the method of split integration steps (Godunov, 1959). Details of the method can be found in Synolakis (2002).

We first simulate the 2004 Sumatra earthquake (Model I), using a composite source consisting of two segments with different fault orientations and focal mechanisms (Table 2). We are motivated by the significant change in the former during the rupture (e.g., Ishii et al., 2005), which affects the far-field directivity of the wave; on the other hand, we did not find it necessary to use a model as detailed as Tsai et al.'s (2005) five-component source, since the tsunami wave in the far field essentially integrates the source as long as it is located on a common fault plane (Okal and Synolakis, 2008). Details of this composite source are given in Table 2; its cumulative moment matches the values obtained by Stein and Okal (2005) and Tsai et al. (2005).

In addition, we carry out similar simulations for potential mega-thrust earthquake sources along the Sumatra subduction zone, featuring different epicentral locations and source geometries, and described by Okal and Synolakis (2008). They are:

- Model II: The 1833 Central Sumatra earthquake, identical to Model I of Okal and Synolakis (2008), and based on the work of Zachariasen et al. (1999) and more recently Natawidjaja et al. (2006);
- Model III: The main 2007 Bengkulu earthquake, based on Borrero et al.'s (2009) simple source with homogeneous slip, as also used by Okal et.al. (2009);
- Model IV: A source releasing the strain left over on the 1833 rupture plane after the 2007 Bengkulu event, similar to Okal and Synolakis' (2008) Model 1a; and
- Model V: A source similar to the latter, but extending south towards the Sunda Straits (Okal and Synolakis' (2008) Model 2*a*).

All relevant parameters of these sources are listed in Table 2.

For each of the sources considered, we use Mansinha and Smylie's (1971) algorithm to compute a static displacement field, which is then interpreted as the initial vertical displacement $\eta(x, y; t = 0_+)$ of the ocean surface. This approximation is classically used and is justifiable as long as the earthquake rupture velocities (typically 2.1 to 2.8 km/s for the 2004 Sumatra event (e.g., Ishii et al., 2005; Tolstoy and Bohnenstiehl, 2005) remain hypersonic with respect to the tsunami propagation velocities (220 m/s for a typical water depth of 5000 m). The simulation is carried out on a 0.1° grid covering the entire Indian Ocean Basin, with a time step δt = 15 s satisfying the classic CFL stability condition (Courant et al., 1925). It is stopped in deep water at the

site of 19 virtual gauges, located at grid points targeted to feature water depths of between 1000 and 1400 m. In this respect, our calculations do not attempt to simulate run-up on individual beaches, which would require full scale bathymetry and topography at each site and is beyond the scope of the present study, but rather they examine the cumulative effect of source geometry and large scale propagation on the tsunami wave available for eventual interaction with small scale bathymetric features.

Figure 7 maps the maximum amplitude reached by the tsunami on the high seas for each of the five models considered, using a common palette which allows for direct comparison between models and locations.

We locate one gauge off each of the four Comoro Islands, and 15 more along other coastlines of the western Indian Ocean basin, mostly offshore of the various international surveys performed to date, but also including a number of large population centres (Beira, Maputo, Durban) deserving of an analysis of hazard from potential future transoceanic tsunamis. We position three gauges along the eastern coast of Madagascar to investigate the significant variation in surveyed 2004 run-up along this geographically regular shoreline (Okal et al., 2006a). All sites are listed by coordinates in Table 3, and mapped on Figure 1.

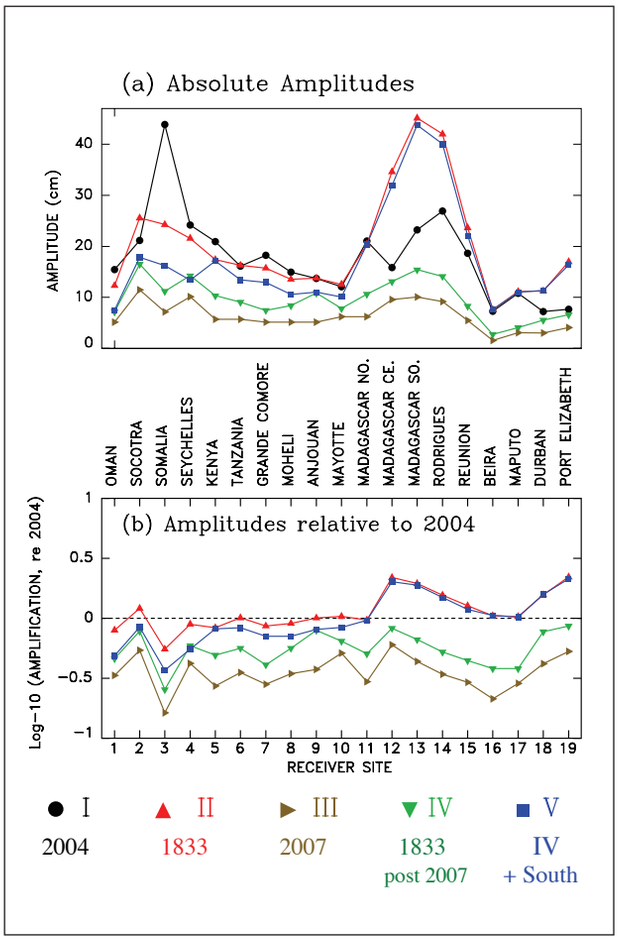

Figure 8. *(**a**) Maximum amplitudes computed at the 19 gauges listed in Table 3 under the five simulated scenarios I to V. (**b**). For scenarios II to IV, the amplitudes in (a) are divided by their values at the same gauge under Scenario I (2004 Sumatra-Andaman tsunami) and the ratio plotted using a logarithmic scale. The dashed line thus represents the amplitude of the 2004 tsunami.*

Results

We first focus on the absolute amplitudes predicted by Model I simulations for the 2004 Sumatra-Andaman tsunami, shown as the black dots on Figure 8a. They are characterised by two peaks, one in Somalia, and one covering Madagascar and the Mascarene Islands (Rodrigues and Réunion). In the absence of deep-water observations of the 2004 tsunami in the Indian Ocean, we caution that any comparison of our simulations with the surveyed dataset must remain qualitative, since the transfer function from deep-water to onland run-up will be highly site-specific and non-linear. This remark notwithstanding, we note that the northern peak qualitatively predicts the large run-up values of up to 9 m surveyed in Somalia (Fritz and Borrero, 2006), which confirms that the exceptional level of destruction in that country was not the effect of site responses, but rather resulted from the peak of source directivity from the second and longest segment of rupture (I.b in Model I).

Within the Comoro archipelago, Model I also correctly predicts maximum amplitudes off Grande Comore, as surveyed above (see Section 2). As for the secondary peak of deep-water amplitudes, we note that our model does predict a local minimum of tsunami amplitudes in the centre of Madagascar, as observed during our field survey, which documented run-up reaching 3.5 m in the north and 5 m in the south, but remaining unobserved in the central part of the coastline (Okal et al., 2006a). Simulated values obtained for Rodrigues and Réunion arenot directly comparable with surveyed run-up because of the different nature of the coastlines (a small reefed island at Rodrigues, a large unreefed Hawaiian volcano at Réunion, versus a continental rectilinear shore in Madagascar).

Simulations for Models II–V are presented both as absolute amplitudes on Figure 8a and as amplitudes relative to Model I on Figure 8b, using a logarithmic scale. The rationale behind this approach is that the site response at an individual beach can be expected to be reasonably independent of the particular wave incident from a common source region, and that comparison of deep-water amplitudes at a common virtual gauge facing the shoreline for two Sumatra source scenarios can therefore give a legitimate, if still somewhat qualitative, insight into the relative amplitudes of run-up on a common nearby beach for those two events.

In this context, Model II (upward-pointing triangles on Figure 8) predicts that the 1833 tsunami should have had amplitudes generally similar to those in 2004 in the northwestern Indian Ocean basin, with the significant

Table 3. Virtual gauges used in the numerical simulations

Number	Coordinates		Location
	(°N)	(°E)	
1	17.45	56.55	Oman
2	12.29	54.61	Socotra, Yemen
3	9.00	51.40	Somalia
4	-4.70	55.30	Seychelles
5	-4.00	40.80	Kenya
6	-6.50	40.30	Tanzania
7	-11.50	43.50	Grande Comore
8	-12.25	43.85	Anjouan
9	-12.05	44.51	Moheli
10	-12.59	45.22	Mayotte
11	-15.00	50.60	Madagascar North
12	-19.60	49.20	Madagascar Central
13	-24.00	47.80	Madagascar South
14	-19.65	63.50	Rodrigues
15	-20.80	55.60	Réunion
16	-20.00	36.50	Beira, Mozambique
17	-26.60	34.00	Maputo, Mozambique
18	-30.10	31.55	Durban, South Africa
19	-34.10	27.00	Port Elizabeth, South Africa

exception of Somalia (smaller in 1833), but larger than in 2004 in the southern part of the basin (Madagascar to South Africa, with the possible exception of the Mozambique sites). As clearly shown on Figure 7, these results express the different azimuth of the lobe of source directivity for the 1833 fault oriented wholly along the Sumatra trench, as predicted from the now classic work of Ben-Menahem and Rosenman (1972). To our knowledge, no historical records for 1833 are available in the Mascarenes, Madagascar, or even South Africa, and thus the only description of the 1833 tsunami in the far field is at the Seychelles, where Jackson et al. (2005) have assessed it as comparable to 2004, in general agreement with our Model II, which is thus given some degree of validation.

By contrast, and expectedly so, the much smaller 2007 Bengkulu earthquake (Model III; right-pointing triangles on Figure 8) generates in most of the basin a tsunami about three to four times smaller than in 1833 (Figure 7). Note that this ratio is less than that of their seismic moments (≈12) since destructive interference due to source directivity is stronger for the larger event. The ratios computed relative to 2004 (typically 0.3; Figure 7b) predict run-up values of 1 m or less at most surveyed sites, in agreement with the fact that the 2007 tsunami went largely unnoticed in the far field, and also more quantitatively, with tide gauge records at Port Elizabeth (Okal et.al., 2009).

In the aftermath of the 2007 Bengkulu earthquake, Model IV (downwards-pointing triangles on Figure 8) involves the release of that portion of the strain accumulated since 1833 which was not released in 2007. As discussed in the Appendix of Okal and Synolakis (2008), recent plate models in the area (Chamot-Rooke and Le Pichon, 1999; Socquet et al., 2006) predict an accumulation of convergence c = 8. 9 m since 1833, i.e., irrespective of the 2007 event, the fault has not yet been loaded back to the level of 1833, when it released 13 m of slip (Natawidjaja et al., 2006). The slip Δu = 6 m used in Model IV is thus a weighted average of the c = 8.9 m presumably available on those sections of fault which did not slip in 2007, and of the ~4 m slip deficiency of the 2007 event with respect to the accumulated convergence c. This slip is available now, and thus Model IV may represent the most probable scenario for a mega-thrust earthquake in south Sumatra in the near future. Should this earthquake not take place before several decades, then its maximum size could in principle grow back to the level of an 1833–type event (albeit reduced by the 2007 release). As would be expected from its intermediate moment value (Table 2), simulations for Model IV suggest far-field amplitudes greater than in 2007, but remaining in all cases smaller than for the 2004 tsunami (Figure 7). However, Figure 8b shows that they come close to matching the 2004 amplitudes in Socotra and South Africa, notably at Port Elizabeth where the impact of the 2004 tsunami was serious, and fell just short of inflicting significant disaster (two casualties at a nearby beach; one car pushed into the harbour and the waves reaching the quays and planks of the main harbour (Okal et al., 2009). Changes in specific conditions, such as a high tide at the time of the tsunami arrival, could render the final run-up at those sites under Model IV greater than in 2004, and thus significant in terms of hazard.

Model V presents a worst-case scenario, which as pointed out by Okal and Synolakis (2008) may not be impossible (notably in the framework of Ando's (1975) observation of the irregularity of fragmentation along large subduction zones), but remains rather improbable given the generally low level of historical seismicity and the absence of known mega-thrust events south of 5°S, as well as our present understanding of heterogeneous coupling at the plate interface (Chlieh et al., 2008). Figures 7 and 8 show that its deep-water amplitudes (plotted as square symbols) are expected to mimic those of the 1833 tsunami, except at the northernmost sites.

This should be of particular concern in Réunion and especially Rodrigues, where Figure 8a suggests deep water amplitudes comparable to those off Somalia in 2004. While these numbers are not directly transposable to expected run-up values, we note the significant damage incurred in 2004 in harbours in Réunion (Okal et al., 2006c) and the general flooding of Port Mathurin in Rodrigues, fortunately and perhaps miraculously without loss of human life. Even a moderate increase in wave amplitude relative to 2004 could result in disastrous consequences in the Mascarene Islands. Large ratios relative to 2004 are also predicted on Figure 8*b* at the South African sites, especially Port Elizabeth, where a possible doubling of wave amplitudes (as suggested under Scenario V) would pose a very serious threat to harbour infrastructure (Okal et.al., 2009).

Conclusion

Our field surveys in the Comoros and Tanzania complement the datasets compiled by the previous ITSTs. They reveal that some of the highest run-up in the western Indian Ocean occurred on the northeastern shores of Grande Comore (6.9 m at Bouni, surpassed only by the catastrophic values in Somalia); however, these values were obtained on shorelines featuring a steep gradient (either natural or engineered in the form of a seawall), and thus the horizontal extent of inundation remained modest and consequently, damage was limited. On the islands of Mayotte and Zanzibar, characterised by a well developed reef system, our surveys yielded relatively scattered values of run-up, which supports the observation, during previous tsunami surveys, that the small-scale details of the reef structure can play a crucial role in controlling the final amplitude of the wave as it reaches the dry land. Finally, our survey on the Tanzanian mainland confirms casualties and suggests that the death toll may have been second only to Somalia among African nations.

Simulation efforts based on a simplified model of the 2004 earthquake source, and limited to propagation on the high seas, correctly predict a number of properties of the cumulative database of run-up values obtained by ITSTs over the past three years. In particular, the exceptional run-up amplitudes in Somalia are explained as resulting mainly from source directivity; the relative amplitudes at the various sites in the Comoros, and the evolution of run-up along the coast of Madagascar are correctly predicted by our simulation, which indicates that these effects result from irregularities in deep water bathymetry, rather than from small-scale site effects.

Simulation of the recent 2007 Bengkulu tsunami correctly predicts its benign effect in the far field, readily attributable to its small moment, relative to genuine mega-thrust events such as the 2004 Sumatra-Andaman earthquake, or the great 1833 Mentawai event. Simulation of the latter based on a model derived from Zachariasen et al.'s (1999) study of emerged coral structures confirms its lone transoceanic report in the Seychelles, but also indicates that its far-field distribution should have featured significant differences with that of the 2004 tsunami, due mainly to a different orientation of the main source, and hence of its directivity lobe. In particular, the Mascarene Islands (Rodrigues, Réunion, and presumably Mauritius) should have suffered a significantly greater tsunami in 1833 than in 2004.

Because it provides a direct comparison of the various scenarios with the 2004 tsunami – the only one for which there exists a comprehensive database of run-up measurements – Figure 8b can be used to draw direct inferences on tsunami hazard along the western shores of the Indian Ocean under a number of scenarios of variable expectability. Under the most probable scenario (Model IV), deep water amplitudes are generally predicted below their levels in 2004, but come dangerously close to matching them at a number of locations, notably Socotra (which had experienced damage at its eastern end in 2004) and most importantly, Port Elizabeth, South Africa, where harbour infrastructure could be at risk. Finally, the more improbable, but perhaps not impossible, Model V would lead to much larger amplitudes at the southern sites, where they would equal and often surpass significantly those of the 2004 tsunami.

A remarkable aspect of Figures 7 and 8 is that our worst-case scenario, Model V, is predicted to essentially reproduce across the board the deep-water wave field of the 1833 tsunami (except north of Kenya where it remains smaller). The latter could therefore serve as a benchmark for the assessment of future hazard from the Sumatra trench. The 1833 event is mostly undocumented in the western Indian Ocean, which we attribute to the lack of archives, since it was reported in the Seychelles (Jackson et al., 2005), and thus must have affected the entire area. Our work suggests that its run-up amplitudes could have been substantial, as they should have equaled or surpassed those of the 2004 tsunami at most sites. We thus suggest that a programme of paleo-tsunami investigations in the far field could help cast some insight into the 1833 tsunami, and consequently on maximum tsunami risk from future mega-earthquakes at the Sumatra trench. Of particular interest would be sites combining a high run-up value with extended inland inundation, e.g., in estuarine environments, such as Grand Baie, Rodrigues (Okal et al.'s (2006c) site 6), Amdigozabe, Madagascar (Okal et al.'s (2006a) site 1), Xaafuun, Somalia (Fritz and Borrero's (2006) site 23), Hajoho, Anjouan (this study's site 17), and more generally unsurveyed locations in areas such as South Africa, where our study suggests a potential for serious tsunami hazard despite an absence of archived historical records.

Acknowledgments

We thank Hamidi Soule Saadi, Director of the Karthala Volcanic Observatory in Moroni, as well as the University of the Comoros, for logistical help during the 2006 campaign. We are grateful to Majura Songo for help at the mainland Tanzanian sites, and to Emily Okal for assistance during the survey on Zanzibar. The field survey in Tanzania was conducted as part of Professor Eric Calais' programme of cooperative research; we thank the Tanzanian Commission for Science and Technology for granting his group a research permit. The paper benefitted from the comments of two anonymous reviewers. This study was partially supported by the National Science Foundation under Grant CMS-03-01054 to EAO. Additional support from the Howland Fund of the Department of Earth and Planetary Sciences, Northwestern University, and from Commissariat à l'Energie Atomique, France, is gratefully acknowledged. Maps were drafted using the GMT software (Wessel and Smith, 1991).

References

Ando, M. (1975). Source mechanism and tectonic significance of historical earthquakes along the Nankai trough, Japan. *Tectonophysics,* **27,** 119–140.

Ben-Menahem, A. and Rosenman, M. (1972). Amplitude patterns of tsunami waves from submarine earthquakes. *Journal of Geophysical Research,* **77**, 3097–3128.

Borrero, J.C., Weiss, R., Okal, E.A., Hidayat, R., Suranto, Arcas, D., Ji, C. and Titov, V.V. (2009). The tsunami of 12 September 2007, Bengkulu Province, Sumatra, Indonesia: Post-tsunami survey and numerical modeling. *Geophysical Journal International,* **178**, 180–194.

Chamot-Rooke, N. and Le Pichon, X. (1999). GPS-determined Eastward Sundaland motion with respect to Eurasia confirmed by earthquake slip vectors at Sundaland Philippine trenches. *Earth and Planetary Science Letters,* **173**, 439–455.

Chlieh, M., Avouac, J.-P., Sieh, K., Natawidjaja, D.H. and Galetzka, J. (2008). Heterogeneous coupling of the Sumatran megathrust constrained by geodetic and paleogeodetic measurements. *Journal of Geophysical Research,* **113**, *(B5),* B05305, 31pp.

Courant, R., Friedrichs, K. and Lewy, H. (1928). Über die partiellen Differenzengleichungen der mathematischen Physik. *Mathematische Annalen,* **100**, 32–74.

Emerick, C.M. and Duncan, R.A. (1982). Age progressive volcanism in the Comores Archipelago, western Indian Ocean, and implications for Somali plate tectonics. *Earth and Planetary Science Letters,* **60**, 415–428.

Fritz, H.M. and Borrero, J.C. (2006). Somalia field survey after the December 2004 Indian Ocean tsunami. *Earthquake Spectra,* **22**, S219–S233.

Fritz, H.M. and Okal, E.A. (2008). Socotra Island, Yemen: Field survey of the 2004 Indian Ocean tsunami. *Natural Hazards,* **46**, 107–117.

Godunov, S.K. (1959). Finite difference methods for numerical computations of discontinuous solutions of the equations of fluid dynamics. *Matematicheskiy Sbornik,* **47**, 271–295.

Gripp, A.E. and Gordon, R.G. (2002).Young tracks of hotspots and current plate velocities. *Geophysical Journal International,* **150,** 321–361.

Hajash, A. and Armstrong, R.L. (1972). Paleomagnetic and radiometric evidence for the ages of the Comores Islands, west-central Indian Ocean. *Earth and Planetary Science Letters,* **16**, 231–236.

Ishii, M., Shearer, P.M., Houston, H. and Vidale, J.E. (2005). Extent, duration and speed of the 2004 Sumatra-Andaman earthquake imaged by the Hi-net array. *Nature,* **435,** 933–936.

Jackson, L.E., Barrie, J.V., Forbes, D.L., Shaw, J., Mawson, G.K. and Schmidt, M. (2005). Effects of the 26 December 2004 Indian Ocean tsunami in the Republic of Seychelles. *Eos, Transactions American Geophysical Union,* **86**, *(52),* F6–F7, [abstract].

Kent, P.E., Hunt, J.A. and Johnstone, D.W. (1971). The geology and geophysics of coastal Tanzania. *Geophysical Paper,* **6**, *Institute of Geological Sciences (H.M.S.O.)*, London, 101pp.

Mansinha, L. and Smylie, D.E. (1971). The displacement fields of inclined faults. *Bulletin of the Seismological Society of America,* **61,** 1433–1440.

Müller, R.D., Sdrolias, M. Gaina, C. and Roest, W.R. (2008). Age, spreading rates, and spreading asymmetry of the world's ocean crust. *Geochemistry, Geophysics, Geosystems,* **9**, Q04006.

Natawidjaja, D., Sieh, K., Chlieh, M., Galetzka, J., Suwargadi, B., Cheng, H., Edwards, R.L, Avouac, J.-P. and Ward, S. (2006). Source parameters of the great Sumatran earthquakes of 1797 and 1833 inferred from coral microatolls. *Journal of. Geophysical Research,* **111**, *(B6),* B06403, 37pp.

Okal, E.A. (2008). The excitation of tsunamis by earthquakes, *In:* E.N. Bernard and A.R. Robinson (Editors), The Sea: Ideas and observations on progress in the study of the seas. Harvard University Press, United States of America **15,** 137–177.

Okal, E.A. and Hébert, H. (2007). Far-field modeling of the 1946 Aleutian tsunami. *Geophysical Journal International,* **169**, 1229–1238.

Okal, E.A. and Synolakis, C.E. (2008). Far-field tsunami hazard from mega-thrust earthquakes in the Indian Ocean. *Geophysical Journal International,* **172**, 995–1015.

Okal, E.A., Fritz, H.M., Raveloson, R., Joelson, G., Pančošková, P. and Rambolamanana, G. (2006a). Madagascar field survey after the December 2004 Indian Ocean tsunami. *Earthquake Spectra,* **22**, S263–S283.

Okal, E.A., Fritz, H.M., Raad, P.E., Synolakis, C.E., Al-Shijbi, Y. and Al-Saifi, M. (2006b). Oman field survey after the December 2004 Indian Ocean tsunami. *Earthquake Spectra,* **22**, S203–S218.

Okal, E.A., Sladen, A. and Okal, E.A.-S. (2006c). Rodrigues, Mauritius and Réunion Islands field survey after the December 2004 Indian Ocean tsunami. *Earthquake Spectra,* **22**, S241–S261.

Okal, E.A., Fritz, H.M., Synolakis, C.E., Borrero, J.C., Hartnady, C.J.H. and Weiss, R. (2009). 2004 Sumatra tsunami surveys in the western Indian Ocean and inferences for future tsunami hazard in the region. *Processings of the General Assembly of the International Association of Seismology and Physics of the Earth's Interior*, 10-16 January 2009, Cape Town (abstract).

Robertson, A.G., Dwyer, D.E. and Leclercq, M.G. (2005). "Operation South East Asia Tsunami Assist": an Australian team in the Maldives, *The Medical Journal of Australia,* **182**, 340–342.

Socquet, A., Vigny, C., Chamot-Rooke, N., Simons, W., Rangin, C. and Ambrosius, B. (2006). India and Sunda plates motion and deformation along their boundary in Myanmar determined by GPS. *Journal of Geophysical Research,* **111**, *(B5),* B05406, 11pp.

Stamps, D.S., Calais, E., Saria, E., Hartnady, C., Nocquet, J.-M., Ebinger, C.J. and Fernandes, R.M. (2008). A kinematic model for the East African Rift. *Geophysical Research Letters,* **35**, *(5),* L05304, 6pp.

Stein, S. and Okal, E.A. (2005). Size and speed of the Sumatra earthquake. *Nature,* **434**, 581–582.

Synolakis, C.E. (2002) Tsunami and seiche. *In:* W.-F. Chen and C. Scawthron (Editors), Earthquake Engineering Handbook, *CRC Press, Boca Raton, United States of America*, **9**, 1–9.

Synolakis, C.E. and Kong, L. (2006). Runup measurements of the December 2004 Indian Ocean tsunami. *Earthquake Spectra,* **22**, S67–S91.

Synolakis, C.E. and Okal, E.A. (2005). 1992-2002: Perspective on a decade of post-tsunami surveys. *In:* K. Satake (Editor), Tsunamis: Case studies and recent developments*, Advances in Natural and Technological Hazards Research,* **23**, 1–30.

Titov, V.V. and Synolakis, C.E. (1998). Numerical modeling of tidal wave runup. *Journal of Waterway, Port, Coastal, and Ocean Engineering,* **124**, 157–171.

Titov, V.V., Rabinovich, A.B., Mofjeld, H.O., Thomson, R.E. and González, F.I. (2005). The Global Reach of the 26 December 2004 Sumatra Tsunami. *Science,* **309**, 2045–2048.

Tolstoy, M. and Bohnenstiehl, D.R. (2005). Hydroacoustic constraints on the rupture duration, length and speed of the great Sumatra-Andaman earthquake. *Seismological Research Letters,* **76**, 419–425.

Tsai V.C., Nettles, M., Ekström, G. and Dziewonski, A.M. (2005). Multiple CMT source analysis of the 2004 Sumatra earthquake. *Geophysical Research Letters,* **32**, L17304, 4pp.

Weiss, R. and Bahlburg, H. (2006). The coast of Kenya field survey after the 2004 Indian Ocean tsunami. *Earthquake Spectra,* **22**, S235–S240.

Wessel, P. and Smith, W.H.F. (1991). Free software helps map and display data. *Eos, Transactions American*. *Geophysical Union*, **72**, 441 and 445–446.

Zachariasen, J., Sieh, K., Taylor, F.W., Edwards, R.L. and Hantoro, W.S. (1999). Submergence and uplift associated with the giant 1833 Sumatran subduction earthquake atoll: Evidence from coral microatolls. *Journal Geophysical Research,* **104**, 895–919.

Editorial handling: A.A. Nyblade